

Robotic Microassembly and micromanipulation at FEMTO-ST

J. Agnus, N. Chaillet, C. Clévy, S. Dembélé, M. Gauthier, Y. Haddab, G. Laurent, P. Lutz*, N. Piat and M. Rakotondrabe

Received: date / Accepted: date

Abstract This paper deals with a historical overview of the activities of the French FEMTO-ST institute in the field of microrobotic manipulation and assembly. It firstly shows tools developed for fine and coarse positioning: microgrippers, 2 DoF modules and smart surfaces. The paper then goes on the automation of tridimensional microassembly of objects measuring between 10 microns and 400 microns. We are especially focusing on several principles. Closed loop control based on micro-vision has been studied and applied on the fully automatic assembly of several 400 microns objects. Force control has been also analyzed and is proposed for optical Microsystems assembly. At least, open loop trajectories of 40 microns objects with a throughput of 1800 unit per hour have been achieved. Scientific and technological aspects and industrial relevance will be presented.

Keywords Microassembly · Micromanipulation · Microrobotic Automation · MEMS Assembly

1 Introduction

Until now, miniaturization was driven by a general diminution of the volume of the product (e.g. cell phones). Currently, the major objective of the miniaturization is to increase the number of functionalities in a product whose volume is mostly constant (e.g. smart phone). In the future, the functions realized using micro or nanotechnologies would be assembled and packaged in or-

der to build integrated multifunctional products or even intelligent products. The hybridization of technologies in micronanosystems is consequently a major stake for the next ten years. The application fields of these future products are typically the networks of sensors for environmental monitoring or the diagnostic and drug delivery done by intelligent systems embedded in human body. Industrial robotics at this scale should be especially studied in order to propose handling, positioning solutions for automatic assembly of these new generation systems. Since 1995, the research team from Besançon, France, has performed significant research activities in the field of micro and nano robotics. These activities were started since in the LAB-laboratory (Laboratoire d'Automatique de Besançon) and are being continued at FEMTO-ST, where the LAB is integrated in 2008 as the AS2M department (Automatic Control and Micro-Mechatronic Systems Department).

FEMTO-ST/AS2M activities deal with the micromanipulation and microassembly issues. More precisely, FEMTO-ST robotic motions, perception, control and manipulation at the microscale and also new activities at the nanoscale. It corresponds to various and multidisciplinary scientific issues:

- microrobotic and adaptronic systems: systems for feeding, carrying, gripping, micrometer size and microfabricated robotics, strategies for microassembly. Some examples are in [10, 38, 45],
- advanced control of dynamic and complex systems: modelling and control of microactuators microsystems, and smart materials, of discrete or continuous distributed systems, control by exteroceptive sensors notably by vision. Some examples of our works are given in [9, 19, 23, 27, 34, 35, 43, 44, 46, 48, 49],
- micromanipulation and microassembly: characterization of the interactions in the microworld, strate-

FEMTO-ST Institute, UMR CNRS 6174 - UFC / ENSMM / UTBM

Automatic Control and Micro-Mechatronic Systems (AS2M) Department

24, rue Alain Savary, 25000 Besançon, FRANCE

*corresponding author: philippe.lutz@femto-st.fr

- gies for microhandling based on physical principles relevant at this scale (the case of the liquid environment has been particularly studied) [21, 25, 26, 41],
- perception and measurement: measure of microforces and artificial vision [2, 20, 51, 52].

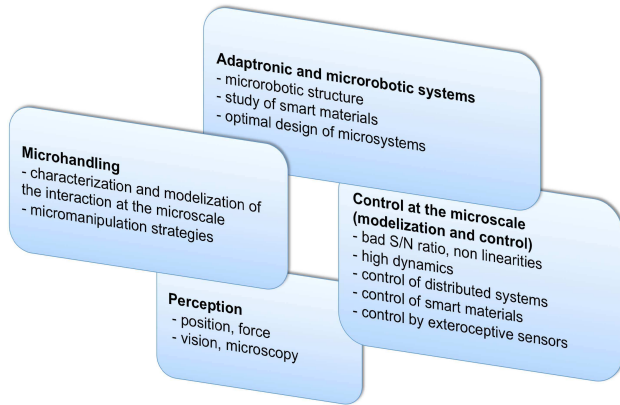


Fig. 1 Major addressed issues studied at FEMTO-ST/AS2M.

Figure 1 summarizes the major addressed issues studied at FEMTO-ST/AS2M. This paper summarizes the activities of the French institute FEMTO-ST in micromanipulation and micro-assembly. First section is devoted to present some tools for micromanipulation and microassembly which have been developed. In second-2 is presented automatic 3D assembly using visual seving on 400 microns objects. An other way to assemble automatically microparts is to use force control as presented in section-3. Teleoperation of the assembly of 40 microns objects are detailed in section-4 before a presentation of the future challenges in micronanoassembly.

2 Tools for micromanipulation and microassembly

2.1 Microgrippers made at FEMTO-ST

The microgrippers, developed at FEMTO-ST [37], are based on two degrees of freedom (DOF) bimorphs that allow open-and-close motion as well as up-and-down motion (Figure 2). Each finger is able to move independently from the other in two orthogonal directions. This microgripper, named MMOC (Microprehensile Micro-robot On Chip) has therefore 4 DOF and is able to grip, hold and release submillimetric-sized objects up to several micrometers. The up-and down motion can be useful for fine motion, for release strategies of objects by crossing the fingers or for insertion of microparts and is particularly convenient to align the finger-tips if they

are misaligned after the microfabrication processes and assembly.

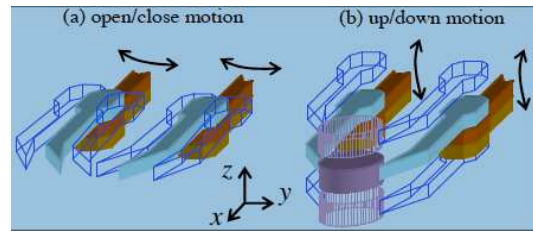


Fig. 2 Mobilities of the microgripper.

The principle of one finger is based on a piezoelectric cantilever with local electrode, named duo-bimorph (Figure 3). Such a microgripper presents at the end of the finger tips for $\pm 100V$ a $320\mu m$ stroke for open/close motion and a $200\mu m$ stroke for up/down motion.

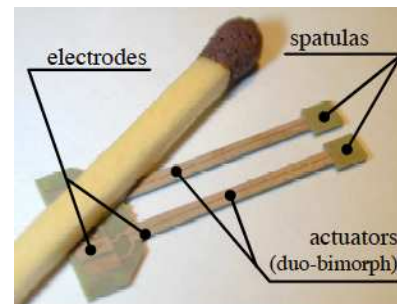


Fig. 3 Piezoelectric actuators of the FEMTO-ST microgripper.

Several packaging have been designed from 2002 to 2012 (Figure 4): the first one, built to illustrate the 'Microrobot on chip' concept (Figure 4-a) has rapidly given way to a more robust plug-and-use microgripper integrated in a LEMO[®] connector (Figure 4-b) for micromanipulation of objects which dimensions are between $100\mu m$ and $1mm$. The version given in Figure 4-c has been designed for compactness reasons to embed the microgripper on a KLEINDIECK's robot (MM3) for micromanipulation in a Scanning Electron Microscope (SEM). The last version (figure 3d) allows several developments, including finger-tips improvement and integration of position and force sensors. It is able to manipulate objects which sizes are between $10\mu m$ and $100\mu m$.

Beyond its performances and its four degrees of freedom that make this FEMTO-ST microgripper particularly efficient, the success of a micromanipulation is often conditioned by the end-effectors. In most of the microgrippers, actuators and end-effectors are both made on the same element. The microgripper developed at

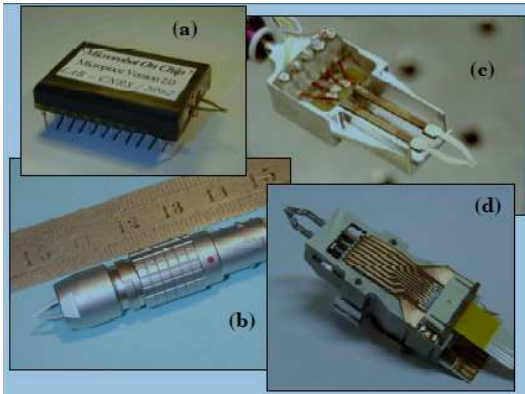


Fig. 4 FEMTO-ST microgrippers along the years.

FEMTO-ST is composed of an actuator and a connection system to fix end-effectors. The two piezoelectric actuators have two spatulas (Figure 3) where different kinds of finger-tips can be fixed. An automated fixing system, with removable thermal glue has already been studied [3]. This microgripper is then particularly flexible to support any end-effector design.

Indeed, the size, the shape, the materials in contact and the environment conditions are some important parameters to achieve a good micromanipulation. These parameters must be adapted to the objects manipulated. The finger-tips material must be also choice for the expected application (conductive finger-tips, transparent, biocompatible, etc).

We designed several end-effectors to match each application. For instance, the first prototypes were equipped with Nickel finger-tips with $200\mu\text{m}$ in thickness micro-fabricated by a LIGA-UV process. Figure 5 shows different shapes. They allowed to easily handle objects between $100\mu\text{m}$ and more.

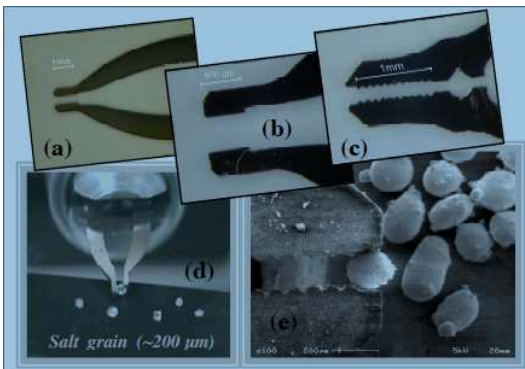


Fig. 5 Nickel finger-tips ($200\mu\text{m}$ thick).

The environment conditions are also critical at this scale because of the complex force gradients due to adhesion forces (surface tension forces, electrostatic forces

and Van der Waals atomic forces). Below $100\mu\text{m}$, many problems arise, especially during the release phase, due to the surface forces between the end-effectors and the manipulated object. Specific silicon end-effectors able to grasp objects between $10\mu\text{m}$ and $100\mu\text{m}$ have been designed (Figure 6). They were microfabricated mainly with DRIE process on SOI wafer with $10\mu\text{m}$ for the handle thickness. The gap and the alignment of the tips are provided by breakable-parts broken after gluing the pair of fingers on the spatulas of the actuators (Figure 6-a and -b). Figure 3-b and -c show respectively the manipulation of a $20\mu\text{m}$ silicate grain and $100\mu\text{m}$ glass sphere.

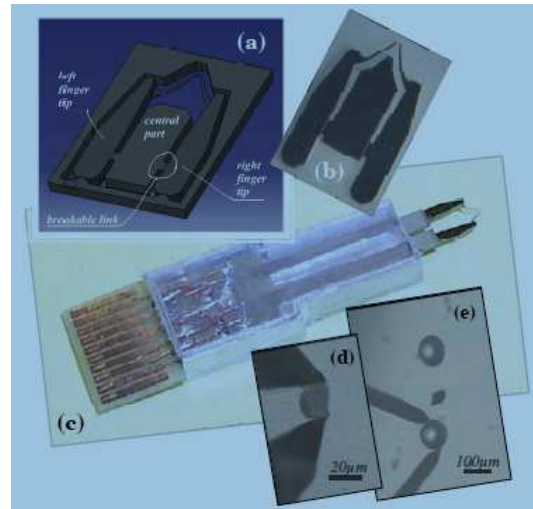


Fig. 6 Silicon finger-tip ($10\mu\text{m}$ thick).

Several research activities in the field of microgripping tools are currently under development concerning in particular some sensorized finger-tips based on piezoresistive effect. It measures grasping forces and enables the control in force and/or position of the fingers, based on self-sensing technique [31] [32]. The presented FEMTO-ST microgripper is now commercially available for purchase at the start-up PERCIPIO ROBOTICS [1] end of the research team. The so-called PiTweez (Figure 7) is able to mechanically grasp micro parts between $100\mu\text{m}$ and 1mm . PERCIPIO-ROBOTICS proposes various options with high resolution sensors to increase the accuracy of finger positioning or can design any fingers on demand with a great range of materials according to the user needs. For instance, Figure 8 shows polymer finger-tips designed by PERCIPIO-ROBOTICS to manipulate objects measuring a few tens of micrometers.

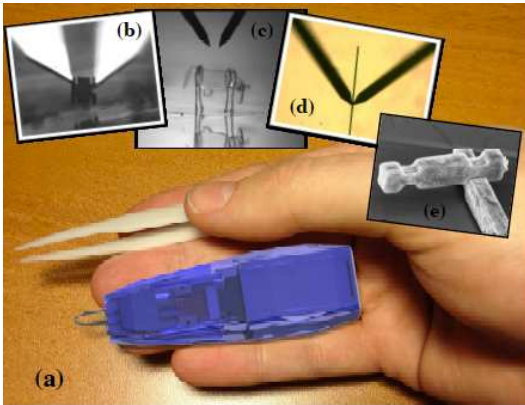


Fig. 7 (a) PiTweez from PERCIPIO-ROBOTICS, (b) micromanipulation of a silicon micro part $40\mu\text{m} \times 40\mu\text{m} \times 5\mu\text{m}$, (c) polymer micro-cow to demonstrate micro-assembly ($500\mu\text{m}$ long, smallest nose part is $50\mu\text{m} \times 50\mu\text{m} \times 5\mu\text{m}$), (d) fiber, $7\mu\text{m}$ diameter, (e) silicon parts assembly, $7\mu\text{m}$ width.

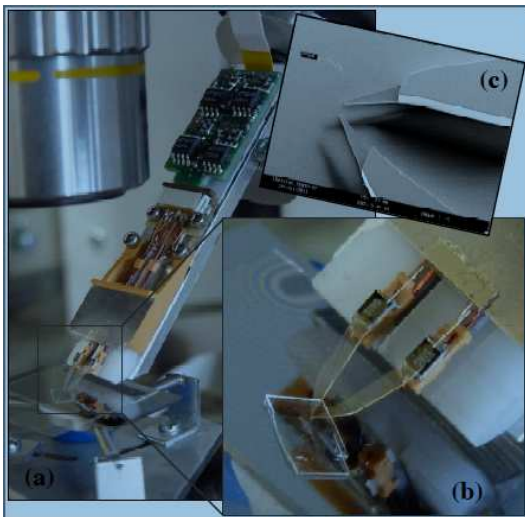


Fig. 8 (a) PiezoTweezer prototype, (b) and (c) details of polymer finger-tip.

2.2 The 2 DOF high stroke and high resolution microrobot: TRING-module

The manipulation and assembly of small components and MEMS may require a system that is able to perform a long distance and a high resolution/precision at the same time. Picking a small component from one location, transporting and placing it in another location for assembly needs that the transportation system have micrometric or submicrometric precision and often more than a ten of millimeters of distance to cover. A way to reach such performances is the use of stepper microrobots often based on stick-slip motion principle. In this section, we present the TRING-module stick-slip microrobot and its use for pick-and-place tasks in microassembly of MEMS at FEMTO-ST.

2.2.1 Kinematic and principle of motion of the TRING-module

The TRING-module is a microrobot that has 2 DOF: linear motion along the axis of its support and angular motion about the same axis (Figure 9). The axis that supports the microrobot is a cylindrical glass. A cantilever is placed at the extremity of the TRING-module and is used as end-effector that facilitates the handling of the manipulated objects. Developed in the previous work [45], its principle of movement is based on the stick-slip functioning and uses piezoelectric microactuators described in [8]. The main features of the TRING-module are its theoretical unlimited stroke both in rotation and in translation, the high resolution that it can offer and its good dexterity (rotation and translation).

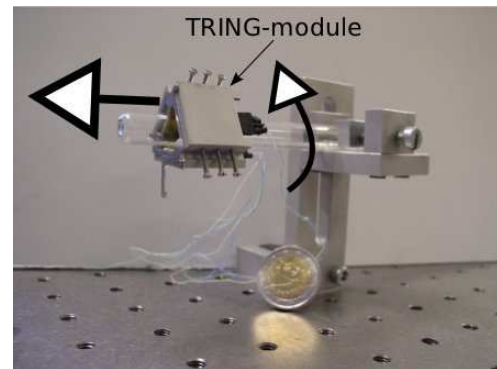


Fig. 9 A photograph of the TRING-module stick-slip microrobot.

2.2.2 Performances of the TRING-module

As a stick-slip microrobot, the TRING-module can perform the high stroke motion by step-by-step. This is obtained by applying a sawtooth voltage to the piezoelectric micro-actuators. The speed of the microrobot is proportional to both the frequency f_{ss} and the amplitude U_{ss} of the voltage, while the step-magnitude depends principally on the amplitude [47]. The high stroke motion is usually employed for a coarse positioning in a large distance. It is also possible to work within a step (sub-step). This sub-step motion, usually employed for fine positioning, is obtained by applying a voltage with limited slope to the microactuators. In sub-step motion, the resolution of the TRING-module is greatly amplified, although the limited range of motion. The step-by-step motion and the sub-step motion can be managed and switched automatically by using the closed-loop control law developed in [47]. The principal advantage of the latter control law is the obtention

of high speed and high precision at the same time without manual reconfiguration of the controller.

Table 1 summarizes the performances of the TRING-module alone without closed-loop control [45] [47]. It clearly shows the high performances, in particular in term of resolution and stroke, of the microrobot that are well suited to the requirement in microassembly in general.

Table 1 Performances of the TRING-module.

Motion	Step	Max speed	Stroke
Linear	70nm → 200nm	2mm/s	unlimited
Angular	17μrad → 44μrad	2.4rpm	unlimited

2.2.3 Pick-and-place tasks based on two TRING-modules

To perform pick-and-place tasks in microassembly, the TRING-module can be used in different ways. One of the main interesting ways is to employ two TRING-modules in the same axis. As pictured in Figure 10, the two microrobots form a microgripper with variable gap between their end-effectors. This scheme allows the manipulation of micro-objects and objects of various sizes. Additionally to that, the transport in large distance and with a high resolution is possible thanks to the performances of the microrobots.

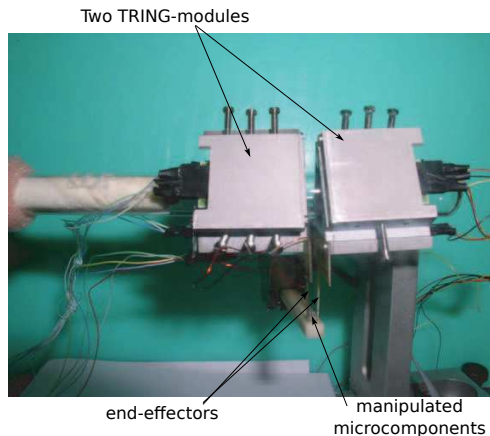


Fig. 10 Two TRING-modules used for pick-and-place tasks in microassembly.

In the configuration pictured in Figure 10, we have proposed to control on force the first TRING-module and to control on position the second one. The main advantage is that additionally to the precise positioning,

the manipulation force and the insertion force (during the assembly) are also commanded in such a way that the destruction of the objects is avoided. It also enables the good gripping of the objects. A pick-and-place task for microassembly based on the two TRING-modules can be splitted into several sub-tasks. The objective of splitting into sub-tasks is to facilitate the control of the two microrobots. They are as follows.

- **Approach:** the two microrobots approach near the object to be manipulated. They are both controlled on position in this sub-task.
- **Picking:** when the microrobots are near the object, one of the two TRING-modules is switched into force control such that its approach is stopped until a given reference force. When this reference force (also called manipulation force) is reached, the picking sub-task is finished.
- **Transport:** after the picking, the object is transported by the two TRING-modules from its initial location to another location. The microrobot controlled on position has as reference input the final location while the microrobot controlled on force has as reference input the manipulation force.
- **Place:** when reaching the final location, the force reference given to the microrobot controlled on force is set to zero. The aim is to release slowly the object.
- **Moving away:** finally, the two microrobots move away from the object in order to completely release the latter. For that, they are controlled on position and their reference inputs correspond to their initial positions.

In Figure 11-a, we present the positions of the two TRING-modules performing a pick-and-place task, x_g being the position of the left microrobot while x_d that of the right one. All along the task, the left microrobot is controlled on position. On the other hand, the right microrobot is controlled on force between the picking sub-task and the place sub-task.

The different experimental results demonstrated the interesting advantages that bring the TRING-module microrobot in microassembly of small objects. In particular, different sizes of objects can be manipulated, their transport from a location to another one for assembly is large and can be done very precisely, and the manipulation force can be controlled in order to avoid the objects destruction and to obtain a good gripping. Finally, the high dexterity (2 DOF) of the microrobot can also be very benefit for pick-and-place and manipulation in the space, instead of only in the plane.

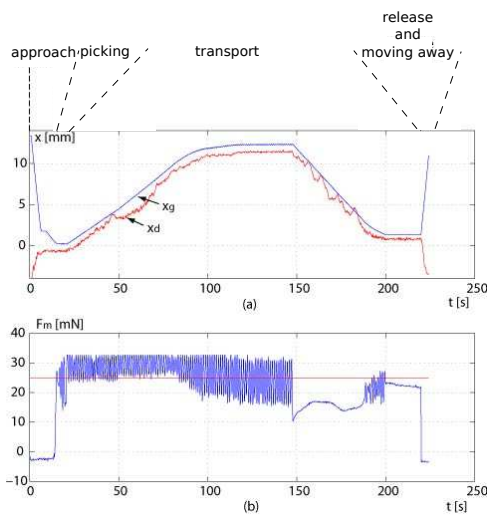


Fig. 11 Evolution of the two TRING-modules performing a pick-and-place task for microassembly.

2.3 Smart Surface

The manipulation without contact is the best way to manipulate clean or delicate objects such as silicon wafers, glass sheets, solar cell or flat foodstuffs. A new principle of aerodynamic traction using induced air flow is proposed to transport and position objects without contact [18], [36]. The induced air flow surface is a 120 mm x 120 mm square surface drilled by two kinds of holes (cf. fig 12). The object is maintained in constant levitation thanks to the air cushion created by the airflow that comes through a common air inlet. The novelty is that the object can be moved on the table by generating strong vertical air jets through specific holes of the surface. These vertical air jets create an induced air flow in the surrounding fluid that pulls the object towards the nozzle (cf. fig 12). Each nozzle is driven by an independent solenoid valve. Thus an object can be transported by opening successively the appropriate valves.

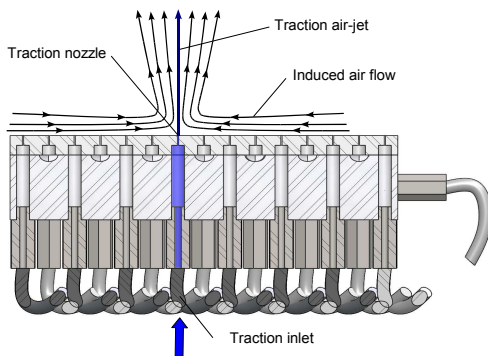


Fig. 12 The induced air flow surface.

The experimental setup for the induced air flow surface is composed of pressurized air supply, two pressure regulators, the set of 56 solenoid valves and its control system, and a computer for vision processing. Fig. 19 describes the complete hardware configuration. The induced air flow surface is put on a mechanical platform to adjust its equilibrium position. Default settings for operating pressures are 15 kPa for levitation and 500 kPa for traction. The valves are independently actuated through a multi-channel digital output board (NI USB-6509) and a 5V/24V amplifier circuit. A camera is used to grab video frames of the surface of the manipulator. The image processing is done by a computer at the rate of 60 frames per second (the software is cvLink).

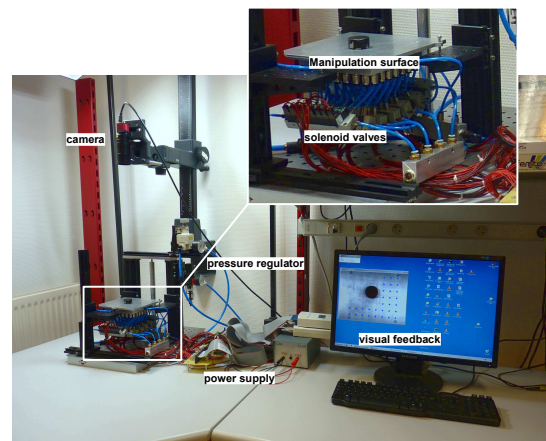


Fig. 13 Overview of the experimental setup.

2.3.1 2 DOF Position Control

A control architecture based on two PID controllers is proposed (see Fig. 14). One PID controls the x -position of the object and the other one controls its y -position. The controllers give respectively the number of y -directed and x -directed lines of air jets to enable and their position(s) relative to the object.

The PID controllers are tuned with the same coefficients, as the distance between two nozzles along

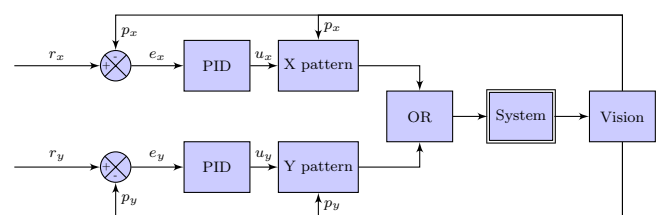


Fig. 14 Control architecture.

the two directions is the same (16mm). The \hat{X} pattern and \hat{Y} pattern blocks calculate the distribution map of the 56 traction nozzles on the surface. They give the position of the nozzles to open depending on the number of y-oriented lines and x-oriented lines to enable and the position of the object. The OR block combines the two patterns using the logical or operator in order to send a unique pattern to the system corresponding to the air jets to enable. The proportional, integral and derivative coefficients of both PID controllers are respectively: $KP = 2$, $KI = 0.15$ and $KD = 1$. They have been tuned by trial-and-error in previous work [18].

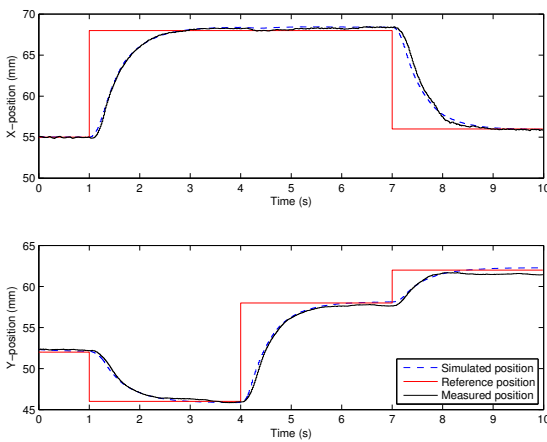


Fig. 15 Experimental results.

2.3.2 Experimental results

Results are shown in Fig. 15. The measured position of the object is compared to the simulated one. The experimental settling time is about 1.5s . Small overshoot (less than 5%) appears sometimes because of the discretization of the control signal and the minimal distance of 8mm between the edge of the object and the nearest sink. The final position of the object varies in a maximal range of $100\mu\text{m}$. We have also experienced tracking: results are shown in Fig. 16. The performances are quite good, but we can note a tracking error of less than 2mm for a speed motion value of 5.03mm/s . Performances in tracking could be improved adapting the controller to this aim. The PID controllers robustness has been evaluated using other objects: the system is stable and gives good performances for different objects.

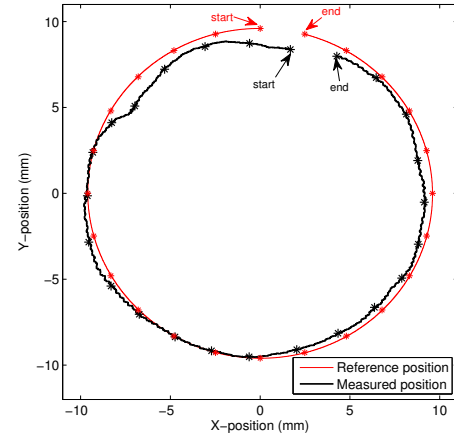


Fig. 16 Target 3D structure at macroscale.

2.4 Conclusion and Future works on the smart surface

The described new contactless transport system for delicate and clean products may be implemented in several industrial production processes, such as semiconductor manufacturing, solar cell production or food industry. The manipulation and object position control have been experimented on the device and gives good performances. Robust controllers are actually implemented on the system to guaranty the stability of the closed loop, to deal with the non linearity of the system and with the different shapes of objects. In the future, more complex tasks could be achieved such as 3-dof positioning, trajectory following, part sorting, etc. We also prospect to miniaturize the device in order to adapt the manipulation principle to millimeter-sized objects (useful in pharmaceutical or watchmaker industries).

3 3D microassembly using visual servoing

3.1 Application

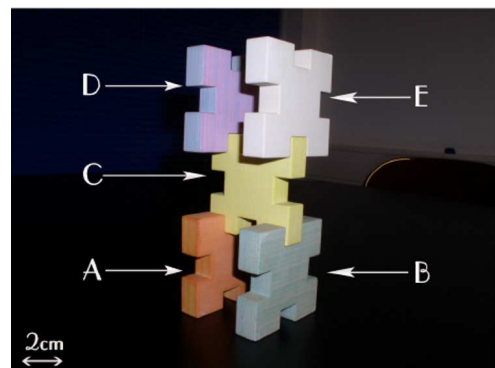


Fig. 17 Target 3D structure at macroscale

The application studied is the assembly of 5 parts by their U-grooves to get stables 3D structures without any use of glue (figure 17). The parts and their grooves measure $400\mu\text{m} \times 400\mu\text{m} \times 100\mu\text{m} \pm 1.5\mu\text{m}$ and $100\mu\text{m} \times 100\mu\text{m} \times 100\mu\text{m} \pm 1.5\mu\text{m}$ respectively leading to an assembly clearance ranging from -3 and $3 \mu\text{m}$. It is a test structure that highlights most of the problems of 3D assembly, notably the need of precision in the control of robot dedicated to the application. This is nothing but the generalization of the assembly of two parts, **A** and **B** for example. The objective is then to automatically insert a groove of **B** into a groove of **A** by means of visual servoing. That objective may be divided into three basic tasks that should be performed in the following sequence: positioning of **A** at the assembly place (task#1), positioning of **B** at the insertion place (task#2) and vertical insertion of **B** into **A** (task#3) (figure 18).

The setup used is positioned inside a controlled envi-

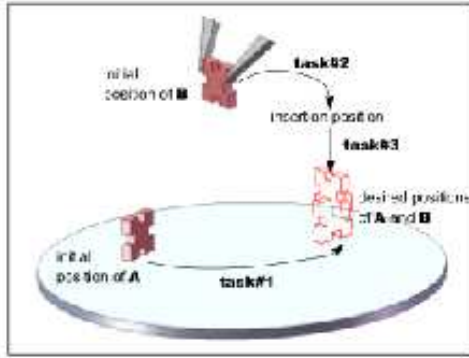


Fig. 18 Objective of the work: insertion of two microparts by their groove

ronment on a vibration-free table (figure 19). It comprises a 5 degree-of-freedom robotic systems distributed into two robots: a $xy\alpha$ robot and a $z\varphi$ robot. The former system (positioning table) is equipped with a compliant support and enables positioning of parts in horizontal plane. The latter system (manipulator) supports the gripper and enables vertical positioning and spatial orientation of microparts. The microhandling system is a 2-finger gripper with 4 degree-of-freedom (2 per finger) as described in ([4]). The imaging system comprises two photon videomicroscopes, but only the one positioned at an angle of $\pi/4$ rad from horizontal plane is used in order to ensure the best perspective view during the assembly tasks. According to the references [53], [5], [22] and [50] it can be described by the linear perspective model whose parameters are determined using a 2D calibration rig.

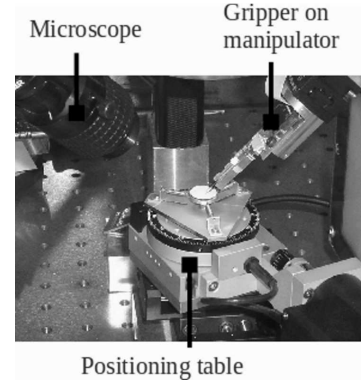


Fig. 19 Assembly setup

3.2 Developed solution

Let $R_C, R_A, R_{A*}, R_B, R_{B*1}$ and R_{B*2} be the frame attached to the camera (i.e. the videomicroscope), the current and final frames of the micropart **A**, the current, insertion and final frames of the micropart **B**, respectively (figure 20). A CAD model of the microparts

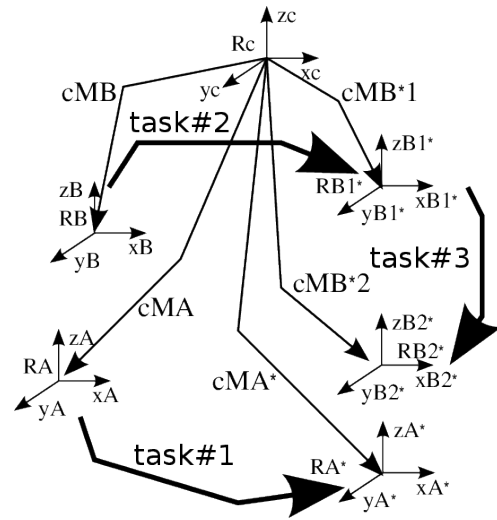


Fig. 20 Diagram of the insertion of part **B** into **A**

based tracking from ([11]) is used. It provides, for each new image, the following information:

- cM_A , the homogeneous transformation between the camera frame and the current position of **A**,
- cM_B , the homogeneous transformation between the camera frame and the current frame of **B**.

Let

- ${}^cM_{A*}$ be the homogeneous transformation between the camera frame and the desired frame of **A**,
- ${}^cM_{B*1}$ be the homogeneous transformation between the camera frame and the insertion frame of **B**,

– ${}^c\mathbf{M}_{B*2}$ be the homogeneous transformation between the camera frame and the desired frame of \mathbf{B} .

They are obtained either in tele-operated mode (using a joystick) or directly from the CAD model.

Let R_F be the base frame of the workcell. The homogeneous transformation between the camera frame R_c and the workcell frame R_F is noted ${}^F\mathbf{M}_A$ and is computed for each object pose.

For each task the regulation to zero of the error \mathbf{e} defined from ${}^i\mathbf{M}_{*i}$ consists of choosing $s = ({}^F t_i, \theta u)$ as the current 3D pose and $s^* = ({}^F t_{i*}, 0)$ as the desired pose of the micropart i , respectively:

$$\mathbf{e} = ({}^F t_i - {}^F t_{i*} \ \theta u) \quad (1)$$

The corresponding control law defined by the exponential decrease of the error is then:

$$\begin{pmatrix} v \\ \omega \end{pmatrix}_F = -\lambda \begin{pmatrix} \mathbf{I}_{3 \times 3} & \mathbf{0}_{3 \times 3} \\ \mathbf{0}_{3 \times 3} & \mathbf{J}_\omega^{-1} \end{pmatrix} (s - s^*) = -\lambda \begin{pmatrix} {}^F t_i - {}^F t_{i*} \\ {}^F \mathbf{R}_i \theta u \end{pmatrix} \quad (2)$$

The task 1 involves the control of the $xy\alpha$ table as:

$$\begin{pmatrix} v_x \\ v_y \\ \omega_\alpha \end{pmatrix}_F = -\lambda_1 \begin{pmatrix} {}^F t_x - {}^F t_{x*} \\ {}^F t_y - {}^F t_{y*} \\ {}^F \mathbf{R}_A \theta u_\alpha \end{pmatrix} \quad (3)$$

The task 2 involves the control of the $xy\alpha$ table as:

$$\begin{pmatrix} v_x \\ v_y \\ \omega_\alpha \end{pmatrix}_F = -\lambda_2 \begin{pmatrix} {}^F t_x - {}^F t_{x*} \\ {}^F t_y - {}^F t_{y*} \\ {}^F \mathbf{R}_B \theta u_\alpha \end{pmatrix} \quad (4)$$

The task 3 involves the control of the $z\varphi$ manipulator as:

$$\begin{pmatrix} v_z \\ \omega_\varphi \end{pmatrix}_F = -\lambda_3 \begin{pmatrix} {}^F t_z - {}^F t_{z*} \\ {}^F \mathbf{R}_A \theta u_\varphi \end{pmatrix} \quad (5)$$

The terms λ , λ_1 , λ_2 and λ_3 are the gains enabling the modulation of the decrease speed.

3.3 Results and discussions

Figure 21 shows some SEM (scanning electron microscope) images of the final assembly. The obtained mechanical play is about $3\mu\text{m}$ showing the relevance of the tracking to deliver high quality pose measurement compatible with microassembly. The final positioning and orientation errors are $3.5\ \mu\text{m}$ and 0.3×10^{-2} rad respectively.

The approach works despite partial occlusions of parts and blurred images (because of the small depth of field of the microscope).

The assembly is performed successively 10 times, it

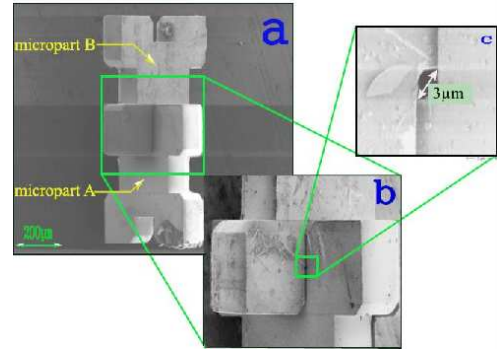


Fig. 21 Some images of the assembled structure from a scanning electron microscope

takes an average of 41s with a standard deviation of 3s.

Figure 22 shows some images of the final assembly of 5 parts and some steps: a right and stable structure is obtained without any use of solidating effect.

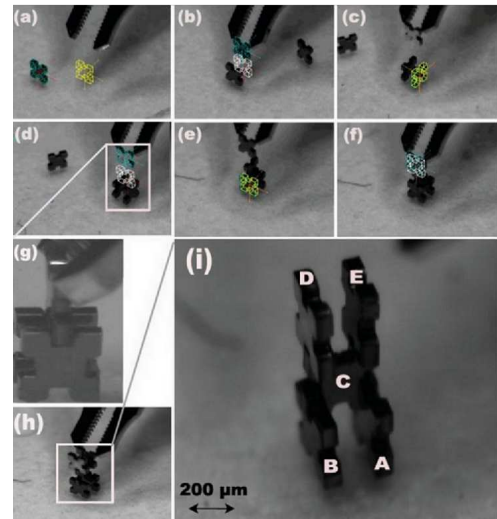


Fig. 22 Assembly of five parts on three levels.

4 Microassembly of MOEMS using force control

4.1 Force guided micro-assembly tasks based on active gripping

Using some micro-assembly processes on force control is a relevant but complex approach. On the one hand, force sensing brings high dexterity which is all the more important at the micro scale than macro one: Indeed micro scale assembling suffers from surface force predominance, difficulties of other sensing alternatives (vision are huge sensors for example) but also lack of

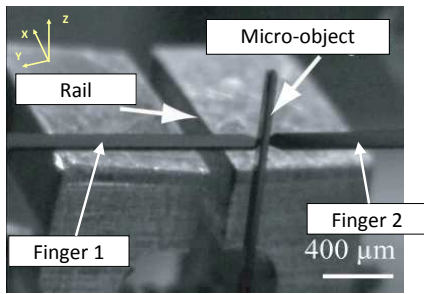


Fig. 23 Guiding task: a micro-object is held between two fingers of a microgripper and guided in the rail.

knowledge. Reversely, on the second hand, force sensors have to be very small to be closely integrated to the contacts (handled micro-object and fingers of the microgripper for example) to ensure good quality of measurement and to measure force of some hundreds of Micro-Newtons. Very few technologies are today available to enable such sensors development.

Based of that statements, two force sensors from femtotools (Switzerland) were integrated to form a microgripper. This microgripper thus provides the measured contact force between finger 1 and the components but also between finger 2 and the same component. Such a microgripper can be used to perform automated cycles including pick, motions and place tasks. Fig. 24 displays the experimental set-up used to perform a guiding task (guiding of the micro-object along a rail). During such a task, contacts between the micro-object and the rail happens when moving the microgripper along the rail axis (X). These contact forces can be estimated through the information sensed by force sensors and a behavioral model of the whole microgripper (force sensors, micro-object subjected to a lateral (Y) force) [39]. Based on this estimation, the force control along Y is ensured [40]. Fig. 24 displays the forces and position during such a guiding task. Based on this principle, automated force control guiding tasks were ensured for the first time with good stability and robustness [40] [42].

4.2 Assembled Micro-Optical Benches

Micro-assembling recently known huge progresses (such as displayed in previous section) making it extremely relevant to be applied on MOEMS prototyping. Indeed, micro-assembly enables to combine in the plane or out of plane several chips issued from different and incompatible microfabrication processes. This is often the case for MOEMS to ensure good enough optical performances.

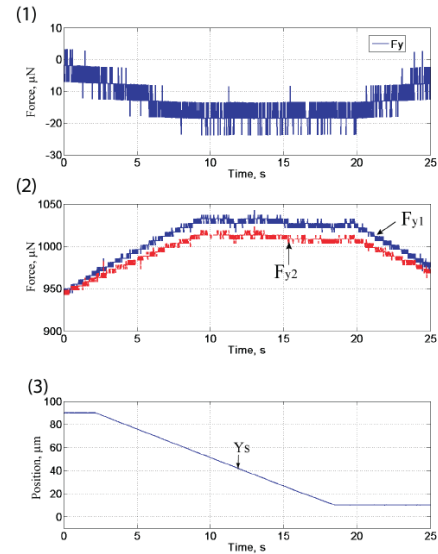


Fig. 24 Forces acting during a guiding task: (2) are the measured contact forces between micro-object and finger 1 and 2 (1) is the contact force between micro-object and rail and (3) is the positioning of the micro-object along the rail.

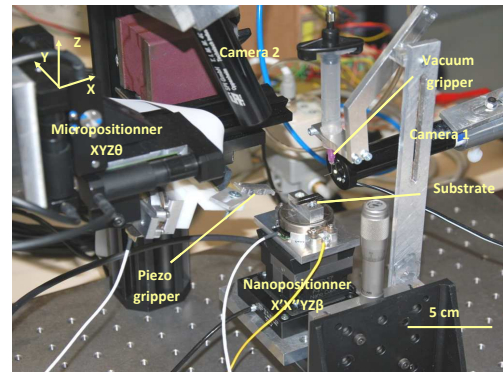


Fig. 25 Micro-assembly cell comprising one 4 DOF piezo-electric microgripper, two robotized arms split onto 9 DOF (micropositionner and nanopositionner), one vacuum gripper and two high magnification cameras.

In the present case, active (based on active material) microgripping is used which is an extremely interesting approach because it enables to adapt the relative position of 2 components during the assembly process (through accurate control) but also to ensure high contact forces in a reversible way. A micro-assembly station has been developed (Fig. 25) to ensure the assembly of RFS-MOB (Reconfigurable Free Space Micro-Optical Bench) Fig. 26. RFS-MOB is composed of a set of several kinds of Silicon components that have been designed to be easily and accurately manipulated and assembled onto a baseplate [6]. Each holder possesses one

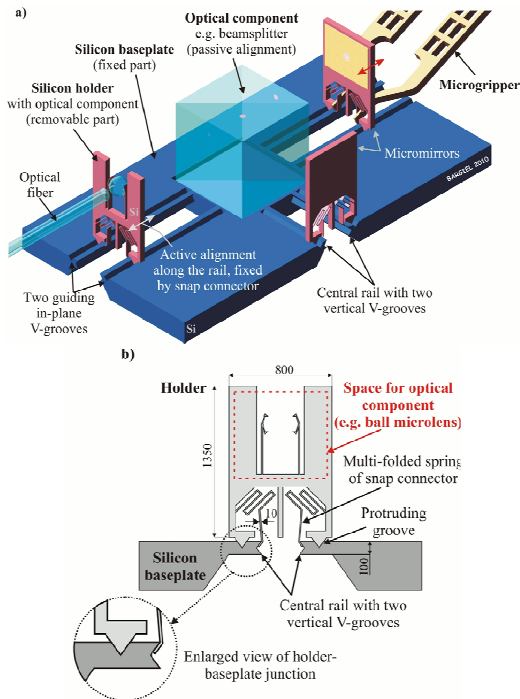


Fig. 26 Assembled RFS-MOB: (b) Every holder possesses one optical functionality and is assembled onto a substrate. It's positioning accuracy is ensure thanks to a V-groove system whereas its holding is done by springs. (a) Such emelentary assemblies can be combine onto the substrate to achieve complex optical functionalities.

optical property (some are micromirrors, others have ball lens or beam splitter for example). Assembly of each holder onto the substrate is done using an active (piezo driven) microgripper. Fig. 27 Displays one example of assembled RFS-MOB comprising 3 holders assembled onto the substrate [33].

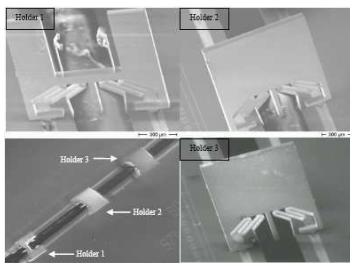


Fig. 27 Assembled RFS-MOB composed of three holders all are aligned along one optical path.

4.3 Positioning accuracy achieved

Previous section shown that complex micro-assemblies can be performed but obtaining good and suitable positioning accuracy is at the same time a very important challenge and required information from an optical performances point of view. To ensure the best positioning accuracy, a specific V-Groove design has been proposed. Each holder has two male V-grooves perfectly fitting with female V-rails fabricated into the baseplate (Fig. 26-b). A system based on small springs then enables to hold the holder onto the baseplate once micro-assembly performed.

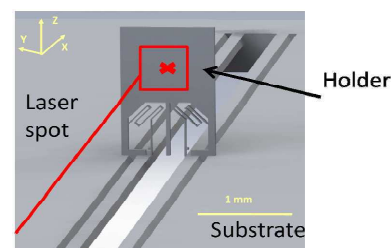


Fig. 28 Laser based scanning of a holder to characterize its positioning accuracy relative to the substrate.

To characterize the positioning accuracy of one holder relative to its substrate, a laser based scanning is performed after micro-assembling (Fig. 28) [33]. The gripping principle used being based on active gripping, it is then possible to adapt the position of the holder to improve its positioning accuracy. Several sets of micro-assembling processes were performed [7]. During each set, 10 different positionng were performed and shown that a positioning accuracy better than the micron (along X) and better than 0.1\AA° around Y and Z can be ensured.

5 Teleoperated assembly of 40 microns objects

The last category of works deals with smaller object whose size is between 10 to 100 microns. At that scale adhesion cannot be neglected and should be taken into account in the design of handling strategies. We are proposing a new reliable and reversible method to position micro-object on a substrate. The principle is an hybrid strategy between adhesion manipulation and gripping. It is based on a hierarchy of forces. In one hand, to guarantee object's release, the adhesion force between object and substrate must be higher than the adhesion force between object and gripper along the normal vec-

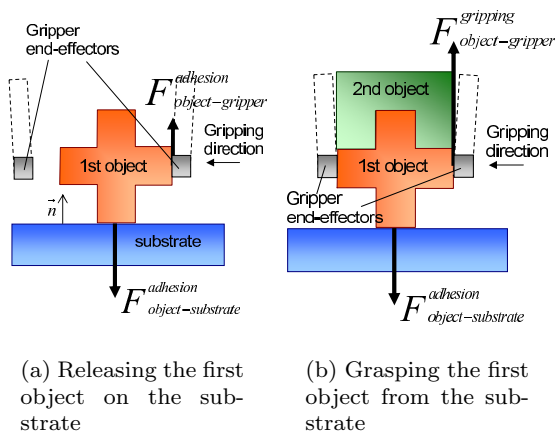


Fig. 29 Principle of the Release and Grasping of the First Object

tor \mathbf{n} of the substrate (see in figure 29(a)):

$$F_{object-substrate}^{adhesion} \gg F_{object-gripper}^{adhesion} \quad (6)$$

To reduce the impact of external perturbations, $F_{object-gripper}^{adhesion}$ must be lower as possible and $F_{object-substrate}^{adhesion}$ must be higher as possible. The major drawback of this release method is the difficulties to grasp the object on the substrate [28]. A reliable grasping cannot be obtained by using only the adhesion force of the gripper. This method is a good way to release the object but not for grasping.

In other hand, to grasp the object, a gripping force higher than the adhesion force between substrate and object along the direction \mathbf{n} is required (see in figure 29(b)):

$$F_{object-gripper}^{gripping} \gg F_{object-substrate}^{adhesion} \quad (7)$$

One of the best technological solution is to use gripper with two fingers where the gripping force could be easily higher than adhesion between the object and the substrate.

Our hybrid method uses advantages of both adhesion manipulation and gripping. It induces a reliable release and grasping of micro-object. To guarantee, the conditions (6, 7), the gripper must have a high ratio between its gripping force and the adhesion force 'object-gripper'.

As presented in figure 29, two ways have been chosen to guarantee first object's manipulation: increase adhesion forces between the substrate and the object and decrease adhesion force between the object and the gripper.

We choose to use as substrate a transparent gel film well-known in microelectronics: Gel-Pak. This material is in fact transparent and softly adhesive, it consequently allows accurate pick and place tasks. Moreover,

the low mechanical stiffness of this polymer induces natural compliance of the substrate required for micro-assembly. In a second time, efforts have been made on end-effectors shaping. First, surface in contact with the micro-object has been reduced by using end-effectors with a small thickness. In second time, the fabrication process called DRIE have been used to give the gripping surface a specific texture. Etching anisotropy of this process is made by a short succession of isotropic etching/protection cycles. These cycles create a phenomenon called *scalloping* illustrated in figure 30. In this way, contact shape between object and end-effectors is a succession of microscopic contact points. The roughness induced by DRIE is able to highly reduce pull-off force. As presented in figure 31, nanostructurations or chemical fonctionnalisations can also be used to reduce the adhesion on the gripper end-effectors [14–17].

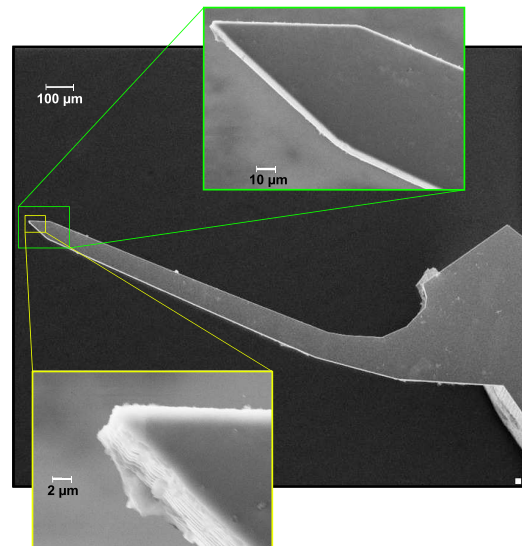


Fig. 30 End-effectors' shape in SEM view. Scalloping is visible in lower picture.

5.1 Experimental set-up

The experimental set-up is based on the piezoelectric gripper presented above. Several kind of finger tips can be glued on this piezoelectric actuator. The finger tips [3, 29] used for micro-assembly have been designed to handle microscopic objects. They are build in single crystal silicon SOI wafer by a well-known microfabrication process: DRIE. These end-effectors have a long and thin beam ($12 \mu m$) designed to handle objects from $5 \mu m$ to few hundred micrometers.

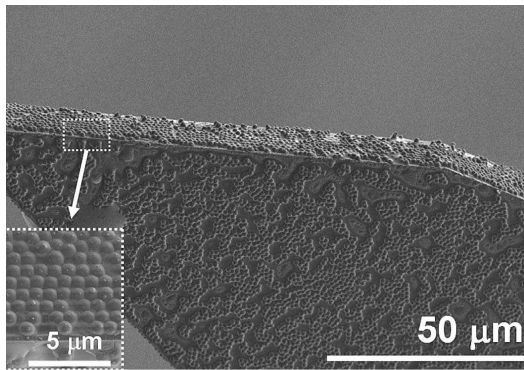


Fig. 31 Nanostructuring of End-effectors' shape (collaborative works between FEMTO-ST and EMPA Institute, Thun, Switzerland) [14]

Testing micro-assembly needs micro-objects that could be mechanically fastened to the others. Thus, micro-objects have been designed with mechanical fastener structures already studied in [13]. To supply a challenging benchmark, objects' shape are squares of $40\ \mu\text{m}$ sides with a thickness of $5\ \mu\text{m}$. SOI wafers of $5\ \mu\text{m}$ device layer thickness and DRIE process have been used to build these microparts [30]. Many shapes, fastener designs and sizes were tested (figure 32). Two kind of parts are presented in this article: the first one is $40\ \mu\text{m}$ square puzzle parts, with four notches of $5\ \mu\text{m}$. The second one is a mechanical plug device between two $40\ \mu\text{m}$ squares. The male part have a key which is able to lock the female part after assembly as proposed by Dechev [13].

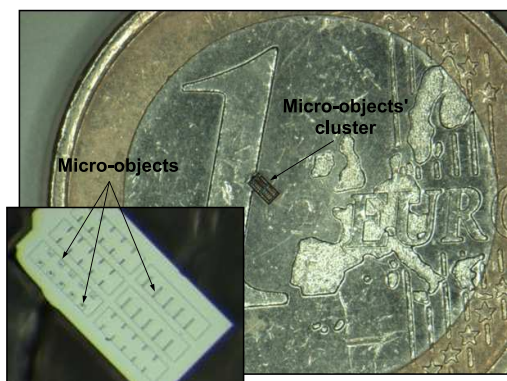


Fig. 32 Micro-objects designed for assembly.

5.2 Results

This approach has been tested in teleoperate mode to assemble benchmark micro-objects. Two kind of mechanical assembly have been tried to make a three-

dimensional microproduct. The first one is made by an insertion of two identical puzzle parts. The second one is a reversible assembly of two different parts.

5.2.1 Insertion

Each puzzle piece has four notches, close to $5\ \mu\text{m}$ width and $10\ \mu\text{m}$ long. As part's thickness is $5\ \mu\text{m}$, assembly of two pieces requires to insert perpendicularly (figure 33).

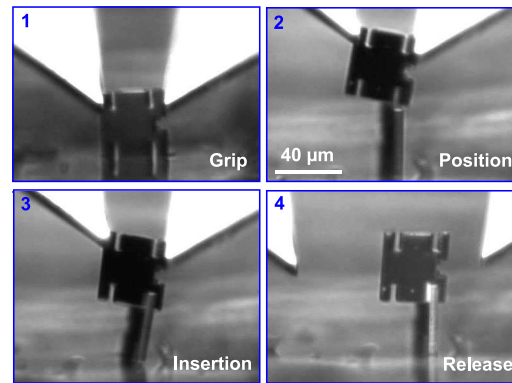


Fig. 33 Insertion assembly.

The first part is gripped and placed vertically on the substrate. The second part is taken vertically too perpendicular to the first one (step 1). Then two puzzle pieces are ready to be assembled. Then the second part is gripped, and is accurately positioned above the first part (step 2). Assembly clearance is very small and evaluated to $200\ \text{nm}$ by SEM measurement and accuracy can be made up by substrate compliance. Indeed, compliance of adhesive substrate allows small rotative motion of the first part thus insertion is easily performed without any fine orientation of the gripper (step 3). When insertion is complete, microgripper is opened to release assembled part (step 4). This last operation can failed when adhesive effects between gripper and puzzle piece are stronger than between both puzzle pieces. In fact, the part stay stucked on the end-effector and opening the gripper disassemble the micro-product. Consequently, the trajectory proposed on section II is used to induce a reliable release.

5.2.2 Reversible Assembly

The second assembly benchmark requires more steps and more accuracy. Both mechanical parts are different but have the same square shape of $40\ \mu\text{m}$ side. The first part have a small key joint with a T shape on one side. The second part have a T shaped imprint in

center of the square (figure 34). To perform assembly, the key must be inserted in the imprint and then a lateral motion of the second part locks the assembly. This benchmark is inspired from Dechev et al [13].

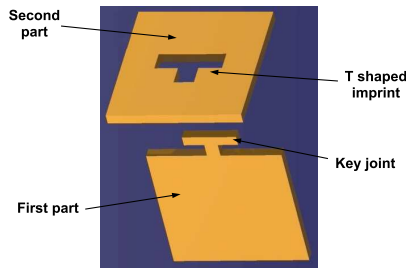


Fig. 34 Lock joint design.

This benchmark has been tested with our robotic structure (figure 35). Parts' orientation is very important, especially for the relative orientation between both micro-objects. The first part is set vertically on the substrate. The gripper is used to grip and align the second part above the key (step 1). When the key is in the imprint (visible on the vertical view), a vertical motion puts the key in the hole (step 2). Finally a lateral motion locks the key and the assembly is performed (step 3).

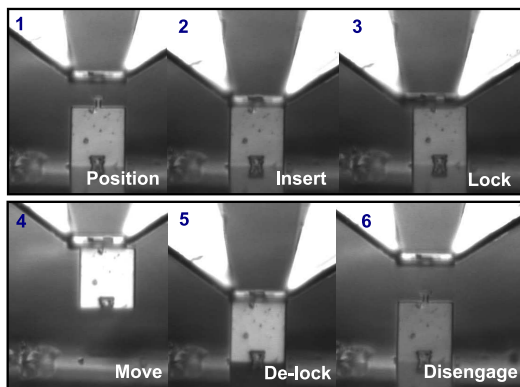


Fig. 35 Reversible assembly.

After locking motion, the 3D microproduct realized can be extracted from the substrate and moved to another place (step 4). Moreover the major interest of this kind of assembly is the possibility to disassemble it. To perform it, motions are repeated on opposite way: a lateral motion to unlock the key (step 5) and a vertical motion to disengage the key from the imprint (step 6). Several cycles of assembly-disassembly have been tested.

5.2.3 Analysis of the reliability

In order to show the reliability of our method, numerous pick and place operations have been performed in teleoperation and in an automatic cycle. The tests have been done on a silicon micro-objects whose dimensions are $5 \times 10 \times 20 \mu\text{m}^3$. The objective of the pick and place operation is to grasp the object placed on the substrate, to move it along $100 \mu\text{m}$ and to release it on the substrate. To evaluate the reliability, the success rate of the pick and place operations and the time cycle have been measured.

First, tests have been done in teleoperation. The operator see the lateral view and the vertical view on two screens. He controls the trajectories and the gripper movements with a joystick without force feedback. 60 operations have been done. The time cycle stays always between 3 and 4 seconds. Secondly, tests have been done in an automatic cycle without force and position feedback. The pick and place trajectory was repeated 60 times and the time cycle was 1.8 seconds.

In both tests, the reliability reaches 100%. As only some articles in the litterature quote the reliability of micromanipulation methods, it is quite difficult to compare this value with other works. However, tests of the reliability of microhandling strategies have been presented in [12,24]. Both tests have been done on polystyrene spheres whose diameter is $50 \mu\text{m}$. The success rate was between 51% and 67% on around 100 tests in [24] and was between 74% and 95% on 60 tests in [12]. Consequently, our method allows a higher reliability on smaller objects which represents a significant contribution.

6 Conclusion

This paper has drawn an overview of the scientific works of FEMTO-ST institute in the automation of 'microassembly' and 'micromanipulation' based on robotic means. We gave three major proposals for microrobotics means which have been developed during the last decade: a piezoelectric microgripper that can move finely grasped objects in two directions and rotation (an industrial version of this microgripper is now on the market), a 2 DoF modules, named TRING-module that can move objet on a long coarse in translation and rotation, and the smart surface we currently studied. The paper proposed several method for the automation of out of plane assembly of objects whose typical size is from 10 microns to 400 microns. Closed loop control based on microvision has been studied and applied on the fully automatic assembly of several 400 microns objects. Force control has been also analyzed and is used for optical

Microsystems assembly. At least, open loop trajectories of 40 microns objects with a throughput of 1800 unit per hour have been achieved. Scientific and technological aspects and industrial relevance have been presented. The research group is now continuing its work on the assembly and manipulation of components and processes of smaller objects. We focus on challenges of assembling components of less than 10 micrometers up to hundreds of nanometers. For this, we develop new strategies to manipulate, new manipulation tools, new methods of control of high precision (integrating the noises for example), integrated microfabricated sensors, ... Micromanipulation and micro-assembly around the micrometer is a key step in the packaging of nanotechnologies and is thus a bottleneck for the advent of nanotechnological products.

7 Acknowledgment

These works have been supported by the French National Agency (ANR) under NANOROL contract ANR-07-ROBO-0003: Nanoanalyse for micromanipulate, and PRONOMIA Contract ANR No. 05-BLAN-0325-01, the European Union under EUPASS contract IST-NMP-1-507978-2: Evolvable Ultra Precision Assembly Systems: Next Generation Technologies for Rapid Deployment of Distributed Ultra Precision Assembly Services for Manufacture of Micro- and Nano-scale Products, HYDROMEL contract NMP2-CT-2006-026622: Hybrid ultra precision manufacturing process based on positional- and self-assembly for complex micro-products, FAB2ASM contract FoF.NMP.2012-3 : Efficient and Precise 3D Integration of Heterogeneous Microsystems from Fabrication to Assembly, and by the Franche-Comté region under the MIAAMI and MIOP Projects and NEMO/Marie-Curie. Authors would like to thank C. Gorecki and S. Bargiel, from the MN2S department of FEMTO-ST for their contribution on MOEMS assembly.

References

1. URL <http://www.percipio-robotics.com>
2. Abadie, J., Piat, E., Oster, S., Boukallel, M.: Modeling and experimentation of a passive low frequency nanoforce sensor based on diamagnetic levitation. *Sensors and Actuators A: Physical* **173**, 227–237 (2012)
3. Agnus, J., Hériban, D., Pétrini, V., Gauthier, M.: Silicon end-effectors for microgripping task. *Journal of Precision Engineering* (2009). DOI doi:10.1016/j.precisioneng.2009.02.005
4. Agnus, J., Nectoux, P., Chaillet, N.: Overview of microgrippers and design of a micromanipulation station based on mmoc microgripper. In: *IEEE International Symposium on Computational Intelligence in Robotics and Automation*, CIRA, Finland (2005)
5. Ammi, M., Ferreira, A.: Haptically generated paths of an afm-based nanomanipulator using potential fields. In: *Proceedings of the 2004 IEEE Nano*. Munich, Germany (2004)
6. Bargiel, S., Rabenoroso, K., Clévy, C., Gorecki, C., Lutz, P.: Towards micro-assembly of hybrid moems components on a reconfigurable silicon free-space micro-optical bench. *Journal of Micromechanics and Microengineering (JMM)* **20** (2010). DOI 10.1088/0960-1317/20/4/045012
7. Bargiel, S., Rabenoroso, K., Mascarob, J.P., Clévy, C., Gorecki, C., Lutz, P.: Technology platform for hybrid integration of moems on reconfigurable silicon micro-optical table. In: *Euroensors XXIV*, Linz, Austria (2010)
8. Bergander, A., Driesen, W., Varidel, T., Breguet, J.: Monolithic piezoelectric push-pull actuators for inertial drives. *IEEE International Symposium Micromechanics and Human Science* pp. 309–316 (2003)
9. Boudaoud, M., Haddab, Y., Gorrec, Y.L.: Modeling and optimal force control of a nonlinear electrostatic microgripper. *IEEE/ASME Transactions on mechatronics* (2012)
10. Chen, Q., Haddab, Y., Lutz, P.: Microfabricated bistable module for digital microrobotics. *Journal of Micro-Nano Mechatronics* **6** (2011)
11. Comport, A.I., Marchand, E., Pressigout, M., Chaumette, F.: Real-time markerless tracking for augmented reality: The virtual visual servoing framework. *IEEE Transactions on Visualization and Computer Graphics* **12**(4), 615–628 (2006)
12. Dafflon, M., Lorent, B., Clavel, R.: A micromanipulation setup for comparative tests of microgrippers. In: *International Symposium on Robotics (ISR)* (2006)
13. Dechev, N., Mills, J.K., Cleghorn, W.L.: Mechanical fastener designs for use in the microassembly of 3d microstructures. In: *Proceedings of ASME IMECE 2004* (2004)
14. Dejeu, J., Benchelany, M., Philippe, L., Rougeot, P., Michler, J., Gauthier, M.: Reducing the adhesion between surfaces using surface structuring with ps latex particle. *ACS Applied Materials & Interfaces* **2**(6) (2010)
15. Dejeu, J., Gauthier, M., Rougeot, P., Boireau, W.: Adhesion forces controlled by chemical self-assembly and ph, application to robotic microhandling. *ACS Applied Materials and Interfaces* **1**(9), 1966–1973 (2009)
16. Dejeu, J., Rougeot, P., Gauthier, M., Boireau, W.: Reduction of micro-object's using chemical functionalisation. *Micronanoletters* (2009)
17. Dejeu, J., Rougeot, P., Gauthier, M., Boireau, W.: Robotic microhandling controlled by chemical self-assembly. In: *Proc. of the IEEE/RSJ Int. Conf. on Robotics and Intelligent Systems*. St. Louis, Missouri, USA (2009)
18. Delettre, A., Laurent, G., Fort-Piat, N.L.: 2-dof contactless distributed manipulation using superposition of induced air flows. In: *IROS2010- IEEE International Conference on Intelligent Robots and Systems*, pp. 2351–2356 (2010)
19. Delettre, A., Laurent, G.J., Haddab, Y., Fort-Piat, N.L.: Robust control of a planar manipulator for flexible and contactless handling. *IFAC International journal of Mechatronics* (2012)
20. Dembele, S., Bert, J., Tamadazte, B., Lefort-Piat, N.: A trifocal transfer based virtual microscope for robotic manipulation of mems components. *Journal of Optomechanics* **4**(4), 342–361 (2010)
21. Dong, W., Rostoucher, D., Gauthier, M.: A novel integrated micro-force measurement system for plane-plane

- contact research. *Review of Scientific Instruments* **81** (2010)
22. Figl, M., Ede, C., Hummel, J., Wanschitz, F., Ewers, R., Bergmann, H., Birkfellner, W.: A fully automated calibration method for an optical see-through head-mounted operating microscope with variable zoom and focus. *IEEE Transactions on Medical Imaging* **Vol. 24, N.11**, 1492–1499 (2005)
 23. Gauthier, J.Y., Hubert, A., Abadie, J., Chaillet, N., LExcellent, C.: Original hybrid control for robotic structures using magnetic shape memory alloys actuators. *IEEE IROS* pp. 747–752 (San Diego CA, Oct-Nov 2007)
 24. Gauthier, M., Lopez-Walle, B., Clévy, C.: Comparison between micro-objects manipulations in dry and liquid mediums. In: *proc. of CIRA'05* (2005)
 25. Gauthier, M., Nourine, M.: Capillary force disturbances on a partially submerged cylindrical micromanipulator. *IEEE Transactions on Robotics* **23**(3), 600–604 (2007)
 26. Gauthier, M., Régnier, S., Rougeot, P., Chaillet, N.: Forces analysis for micromanipulations in dry and liquid media. *Journal of Micromechatronics* **3**(3-4), 389–413 (2006)
 27. Grossard, M., Boukallel, M., Chaillet, N., Rotinat-Libersa, C.: Modeling and robust control strategy for a control-optimized piezoelectric microgripper. *IEEE/ASME - Transactions on Mechatronics (T-mech)* (Aug 2011)
 28. Haliyo, D., Régnier, S.: Manipulation of micro-objects using adhesion forces and dynamical effects. In: *Proceedings of ICRA/IEEE International Conference on Robotics and Automation* (2002)
 29. Heriban, D., Agnus, J., Coudeville, J.R., Gauthier, M., Chaillet, N.: Design of silicon finger tips for a moc (micro-robot on chip) microgripper. In: *Proc. of the Int. Workshop on Topical Meeting on Microfactories (TMMF05)*. Tsukuba, Japan (2005)
 30. Hériban, D., Agnus, J., Pétrini, V., Gauthier, M.: Mechanical de-tethering technique for silicon mems etched with drier process. *Journal of Micromechanics and Micro-engineering* **19**(5), 055,011 (2009)
 31. Ivan, I., Rakotondrabe, M., Lutz, P., Chaillet, N.: Current integration force and displacement self-sensing method for cantilevered piezoelectric actuators. *Review of Scientific Instruments (RSI)* **Vol.80(12)**, 2126,103 (Dec 2009)
 32. Ivan, I., Rakotondrabe, M., Lutz, P., Chaillet, N.: Quasi-static displacement self-sensing method for cantilevered piezoelectric actuators. *Review of Scientific Instruments (RSI)* **Vol.80(12)**, 065,102 (June 2009)
 33. K. Rabenorosoa C. Clévy, S.J.P.M.P.L., Gorecki, C.: Modular and reconfigurable 3d micro-optical benches : Concept, validation, and characterization. In: *International Manufacturing Science & Engineering Conference* (2011)
 34. Khadraoui, S., Rakotondrabe, M., Lutz, P.: Interval modeling and robust control of piezoelectric microactuators. *IEEE - Transactions on Control Systems Technology (T-CST)* (2012)
 35. Kharboutly, M., Gauthier, M., Chaillet, N.: Predictive control of a micro bead's trajectory in a dielectrophoresis-based device. *IEEE IROS* (Oct 2010)
 36. Laurent, G., Delettre, A., Fort-Piat, N.L.: A new aerodynamic traction principle for handling products on an air cushion. *IEEE Transactions On Robotics* **Vol. 29, N.2**, 379–384 (2011)
 37. Lit, P.D., Agnus, J., C. Clévy, N.C.: A four-degree-of-freedom microprehensile microrobot on chip. *Journal of Assembly Automation* **Vol.24, Issue 1**, 33–42 (2004)
 38. Lopez-Walle, B., Gauthier, M., Chaillet, N.: Principle of a submerged freeze gripper for micro-assembly. *IEEE Trans. on Robotics* **24**(4), 897–902 (2008)
 39. Rabenorosoa, K., Clévy, C., Chen, Q., Lutz, P.: Study of forces during micro-assembly tasks using two-sensing-finger grippers. *IEEE/ASME Transactions on Mechatronics* (2012). DOI 10.1109/TMECH.2011.2131673
 40. Rabenorosoa, K., Clévy, C., Lutz, P.: Active force control for robotic micro-assembly: Application to guiding tasks. In: *IEEE ICRA, International Conference on Robotics and Automation* (2010)
 41. Rabenorosoa, K., Clévy, C., Lutz, P., Gauthier, M., Rougeot, P.: Measurement of pull-off force for planar contact at the microscale. *Micro Nano Letters* **4**, 148–154 (2009)
 42. Rabenorosoa, K., Clévy, C., Lutz, P.: Hybrid force/position control applied to automated guiding tasks at the microscale. In: *IEEE/RSJ International Conference on Intelligent Robots and Systems (IROS)* (2010)
 43. Rakotondrabe, M., Clévy, C., Lutz, P.: Complete open loop control of hysteretic, creeped and oscillating piezoelectric cantilever. *IEEE - Transactions on Automation Science and Engineering (T-ASE)* **Vol.7, Issue 3**, 440–450 (July 2010)
 44. Rakotondrabe, M., Gorrec, Y.L.: Force control in piezoelectric microactuators using self scheduled hinf technique. *IFAC - Mech, (Symposium on Mechatronic Systems)* pp. 417–422 (Cambridge Massachusetts USA, September 2010)
 45. Rakotondrabe, M., Haddab, Y., Lutz, P.: Development, modeling, and control of a micro-/nanopositioning 2-dof stick-slip device. *IEEE/ASME - Transactions on Mechatronics (T-mech)* **Vol.14, Issue 6**, 733–745 (December 2009)
 46. Rakotondrabe, M., Haddab, Y., Lutz, P.: Quadrilateral modelling and robust control of a nonlinear piezoelectric cantilever. *IEEE - Transactions on Control Systems Technology (T-CST)* **Vol.17, Issue 3**, 528–539 (May 2009)
 47. Rakotondrabe, M., Haddab, Y., Lutz, P.: Voltage/frequency proportional control of stick-slip microsystems. *IEEE - Transactions on Control Systems Technology (T-CST)* **Vol.16, Issue 6**, 1316–1322 (November 2008)
 48. Rakotondrabe, M., Ivan, I., Khadraoui, S., Clévy, C., Lutz, P., Chaillet, N.: Dynamic displacement self-sensing and robust control of cantilevered piezoelectric actuators dedicated to microassembly tasks. *IEEE/ASME - AIM, (International Conference on Intelligent Materials)* pp. 557–562 (Montreal Canada, July 2010)
 49. Rakotondrabe, M., Rabenorosoa, K., Agnus, J., Chaillet, N.: Robust feedforward-feedback control of a nonlinear and oscillating 2-dof piezocantilever. *IEEE - Transactions on Automation Science and Engineering (T-ASE)* **Vol.8, Issue 3**, 506–519 (July 2011)
 50. Tamadazte, B., Dembélé, S., Fort-Piat, N.L.: A multi-scale calibration of a photon video microscope for visual servo control: Application to micromanipulation. In: *ROSE 2008 - IEEE International Workshop on Robotic and Sensors Environments*, Ottawa, Canada, 17-18 October (2008)
 51. Tamadazte, B., Dembele, S., Lefort-Piat, N.: A multicale calibration of a photon video microscope for visual servo control. *Sensors & Transducers Journal* **5**, 37–52 (2009)
 52. Tamadazte, B., Marchand, E., Dembele, S., LeFort-Piat, N.: Cad model based tracking and 3d visual-based con-

- trol for mems microassembly. *International Journal of Robotics Research* **29**(11), 1416–1437 (2010)
53. Zhou, Y., Nelson, B.J.: Calibration of a parametric model of an optical microscope. *Optical Engineering* **38**(12), 1989–1995 (1999)